Since January 2020 Elsevier has created a COVID-19 resource centre with free information in English and Mandarin on the novel coronavirus COVID-19. The COVID-19 resource centre is hosted on Elsevier Connect, the company's public news and information website.

Research Article

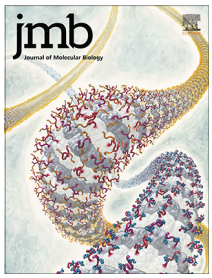

Inhibition of SARS-CoV-2 Infection by Human Defensin HNP1 and Retrocyclin RC-101

Elena Kudryashova [1,2], Ashley Zani [2,3], Geraldine Vilmen [3,4], Amit Sharma [2,3,4], Wuyuan Lu [5], Jacob S. Yount [2,3]* and Dmitri S. Kudryashov [1,2]*

*1 - **Department of Chemistry and Biochemistry,** The Ohio State University, Columbus, OH 43210, USA*
*2 - **Infectious Diseases Institute,** The Ohio State University, Columbus, OH 43210, USA*
*3 - **Department of Microbial Infection and Immunity,** College of Medicine, The Ohio State University, Columbus, OH 43210, USA*
*4 - **Department of Veterinary Biosciences,** College of Veterinary Medicine, The Ohio State University, Columbus, OH 43210, USA*
*5 - **Key Laboratory of Medical Molecular Virology (MOE/NHC/CAMS),** School of Basic Medical Science, and Shanghai Institute of Infectious Disease and Biosecurity, School of Public Health, Fudan University, Shanghai 200032, China*

Correspondence to Jacob S. Yount and Dmitri S. Kudryashov: Infectious Diseases Institute, The Ohio State University, Columbus, OH 43210, USA. *Jacob.Yount@osumc.edu (J.S. Yount), kudryashov.1@osu.edu (D.S. Kudryashov)*
@KudryashovLab (D.S. Kudryashov), @YountLabOSU (J.S. Yount), @AmitSharmaOSU (A. Sharma)
https://doi.org/10.1016/j.jmb.2021.167225
Edited by Alex Compton

Abstract

Severe acute respiratory syndrome coronavirus (SARS-CoV)-2 is an enveloped virus responsible for the COVID-19 pandemic. The emergence of new potentially more transmissible and vaccine-resistant variants of SARS-CoV-2 is an ever-present threat. Thus, it remains essential to better understand innate immune mechanisms that can inhibit the virus. One component of the innate immune system with broad antipathogen, including antiviral, activity is a group of cationic immune peptides termed defensins. The ability of defensins to neutralize enveloped and non-enveloped viruses and to inactivate numerous bacterial toxins correlate with their ability to promote the unfolding of proteins with high conformational plasticity. We found that human neutrophil α-defensin HNP1 binds to SARS-CoV-2 Spike protein with submicromolar affinity that is more than 20 fold stronger than its binding to serum albumin. As such, HNP1, as well as a θ-defensin retrocyclin RC-101, both interfere with Spike-mediated membrane fusion, Spike-pseudotyped lentivirus infection, and authentic SARS-CoV-2 infection in cell culture. These effects correlate with the abilities of the defensins to destabilize and precipitate Spike protein and inhibit the interaction of Spike with the ACE2 receptor. Serum reduces the anti-SARS-CoV-2 activity of HNP1, though at high concentrations, HNP1 was able to inactivate the virus even in the presence of serum. Overall, our results suggest that defensins can negatively affect the native conformation of SARS-CoV-2 Spike, and that α- and θ-defensins may be valuable tools in developing SARS-CoV-2 infection prevention strategies.

Introduction

COVID-19 imposes an extraordinary health threat whose scale and severity can be compared only to that of the Spanish flu pandemic, which raged over a hundred years ago. The COVID-19 pandemic vividly exposed the weakness of the globalized world to new zoonotically transmitted viruses,

Please cite tts article as: E. Kudryashova, A. Zani, G. Vilmen, et al., Inhibition of SARS-CoV-2 Infection by Human Defensin HNP1 and Retrocyclin RC-101Journal of Molecular Biology, https://doi.org/10.1016/j.jmb.2021.167225

which emerge with alarming regularity (e.g., 2003 Severe Acute Respiratory Syndrome coronavirus SARS-CoV,[1] 2009 influenza A H1N1,[2] 2012 Middle East Respiratory Syndrome coronavirus MERS-CoV).[3] Although several effective SARS-CoV-2 vaccines have been generated in an unprecedently short time frame, high levels of transmissibility and mortality of this virus,[4] hesitancy towards vaccination from a large fraction of the world population, and the emergence of variants resistant to vaccine-induced immunity require additional development of non-vaccine therapies against SARS-CoV-2.

Interestingly, despite the high mortality rate, as much as 42% of infected individuals are asymptomatic carriers of SARS-CoV-2,[5–7] suggesting that the virus can be effectively controlled by the human innate immune system.[8] Recently, pro- and antiviral activities of interferon-induced transmembrane proteins (IFITMs) in SARS-CoV-2 infection have been described.[9–11] Likewise, other interferon-stimulated genes, such as CH25H, Ly6E, Tetherin, and ZAP have been demonstrated to have inhibitory effects on SARS-CoV-2 replication *in vitro*.[12–16] Another important and promising class of innate immunity effectors is defensins. These peptides are active against several viruses, including human immunodeficiency virus (HIV), herpes simplex virus, influenza virus, and SARS-CoV.[17–20]

Based on their structural characteristics, mammalian defensins are grouped into three subfamilies called α-, β-, and θ-defensins.[21–25] Humans express α- and β-defensins, while cyclic θ-defensins are produced only by non-human primates.[26] Although human θ-defensin genes are transcribed, a premature stop codon precludes their translation.[27] Intriguingly, human cells retain the ability to produce the cyclic θ-defensin peptides upon transfection of the synthetic "humanized" θ-defensin genes called retrocyclins.[28] Potent antiviral and antibacterial activity[26,29–31] in combination with low cytotoxicity and exceptional stability identified retrocyclins as promising topical microbicides.[32–34]

α-Defensin human neutrophil peptides 1–4 (HNP1-4) are small (~30 a.a.) dimeric cationic amphiphilic peptides produced by neutrophils and stored in azurophil granules.[35] Highly similar HNP1-3 peptides differ from each other only by their first amino acid residue and constitute >98% of the total neutrophil α-defensins.[36] HNP1 shows potent antibacterial,[37–40] antifungal,[41,42] and antiviral activities against enveloped and non-enveloped viruses.[17,18,43] Antiviral mechanisms of defensins[44] are multifaceted, including direct targeting of exposed proteins on viral envelopes and capsids, disruption of viral fusion, inhibition of post-entry processes, or affecting receptors on the host cell surface. Such remarkable versatility is partially explained by the ability of defensins to disrupt membranes,[39] but also by their ability to induce unfolding of metastable proteins, such as bacterial toxins and viral proteins.[45–47] Susceptibility of target proteins to α-defensin-induced unfolding and ultimately inactivation is reliant on their conformational plasticity, which often correlates with thermolability.[48] Near the melting point, proteins exist in equilibrium between folded and partially unfolded states. Unlike the majority of ligands, which bind to folded conformations of protein targets and increase their thermostability, defensins promote unfolding of thermolabile proteins, reducing their melting temperatures.[47] Defensin targets become locked in non-native, partially unfolded, and therefore, non-functional states and cannot undergo necessary conformational transitions and often aggregate/precipitate through exposed hydrophobic surfaces. As evolutionary derivatives of α-defensins,[26] θ-defensins (and retrocyclins, in particular) mainly recapitulate their activity.[49] Defensins are also recognized as chemokines that modulate the immune response by binding to cell surface receptors and interfering with cellular signalling.[44] According to a recent study, enteric human α-defensin HD5 binds to human angiotensin-converting enzyme 2 (a.k.a. ACE2 receptor) on enterocytes obstructing the SARS-CoV-2 Spike binding site, which results in inhibition of SARS-CoV-2 Spike pseudovirus infection.[50] Encouraged by this report, we examined the effects of a neutrophil α-defensin, HNP1, and retrocyclin, RC-101, on SARS-CoV-2 infection. We chose to focus on HNP1, since it is the most relevant α-defensin for respiratory virus infection, as it is produced by neutrophils and is released from their granules at the sites of infection/inflammation. RC-101 replicates most of the α-defensin functions and is a promising candidate for drug development.

Results

HNP1 and RC-101 inhibit SARS-CoV-2 Spike-mediated membrane fusion and pseudotyped virus infection

SARS-CoV-2 homotrimeric Spike glycoprotein binds to the ACE2 receptor on the host cell, mediating membrane fusion and virus entry.[51] Being exposed on the surface of virions, Spike is the main target for virus neutralization by host antibodies. Membrane fusion activity of Spike also enables fusion of Spike-expressing mammalian cells with ACE2-positive cells to form multinuclear cell syncytia.[52] Such syncytia represent a convenient model to study Spike/ACE2 interaction and to test different agents in disrupting this interaction. An additional approach that also does not require biosafety level 3 (BSL3) conditions is to use replication-restricted viruses pseudotyped with SARS-CoV-2 Spike. We initially utilized both systems to test whether HNP1 and RC-101 can interfere with the SARS-CoV-2 Spike interaction with

host cells. Since serum has been shown to negatively affect antipathogen activity of defensins,[40,53,54] we tested their effects in the presence and absence of serum.

Co-transfection of human osteosarcoma U2OS cells with Spike and mCherry promoted their fusion with ACE2-producing human lung Calu-3 cells, leading to multinuclear mCherry-positive syncytia (Figure 1(A) and (B)). In the absence of serum, the addition of HNP1 or RC-101 to the co-culture of Spike- and ACE2-positive cells strongly inhibited syncytia formation (Figure 1(B) and (C)), indicating that defensins are able to inhibit Spike-mediated membrane fusion. Serum largely abrogated the inhibition of syncytia formation by HNP1 (Figure 1(D)), suggesting that abundant serum proteins may compete for defensin binding.

In the next set of experiments, human lung H1299 cells were infected with HIV-based reporter virus-like particles pseudotyped with SARS-CoV-2 Spike (Figure 2(A)); pseudovirus infection was monitored using a secreted NanoLuc luciferase (Nluc) reporter encoded by the virus genome. Pre-treatment of the cells with HNP1 or RC-101 prior to the infection did not affect the pseudovirus infection efficiency (Figure 2(B) and (C)), demonstrating that these defensins did not provide a cell-directed effect on infection. In contrast, one-hour pre-incubation of the pseudovirus particles with the defensins prior to cell infection significantly inhibited the infection (Figure 2(D)). These results suggest that HNP1 and RC-101 can interfere with the viral infection by acting upon the viral particle rather than influencing host molecules (e.g., ACE2 receptor), as it has been suggested for the enteric defensin HD5.[50] As with the Spike-mediated fusion experiments, serum had a negative influence on the inhibitory ability of HNP1 and RC-101 (Figure 2(E)).

HNP1 and RC-101 induce unfolding and precipitation of SARS-CoV-2 Spike protein and inhibit its interaction with ACE2

The results from the SARS-CoV-2 Spike-mediated membrane fusion assays and pseudovirus infections prompted us to test whether HNP1 can directly interact with Spike

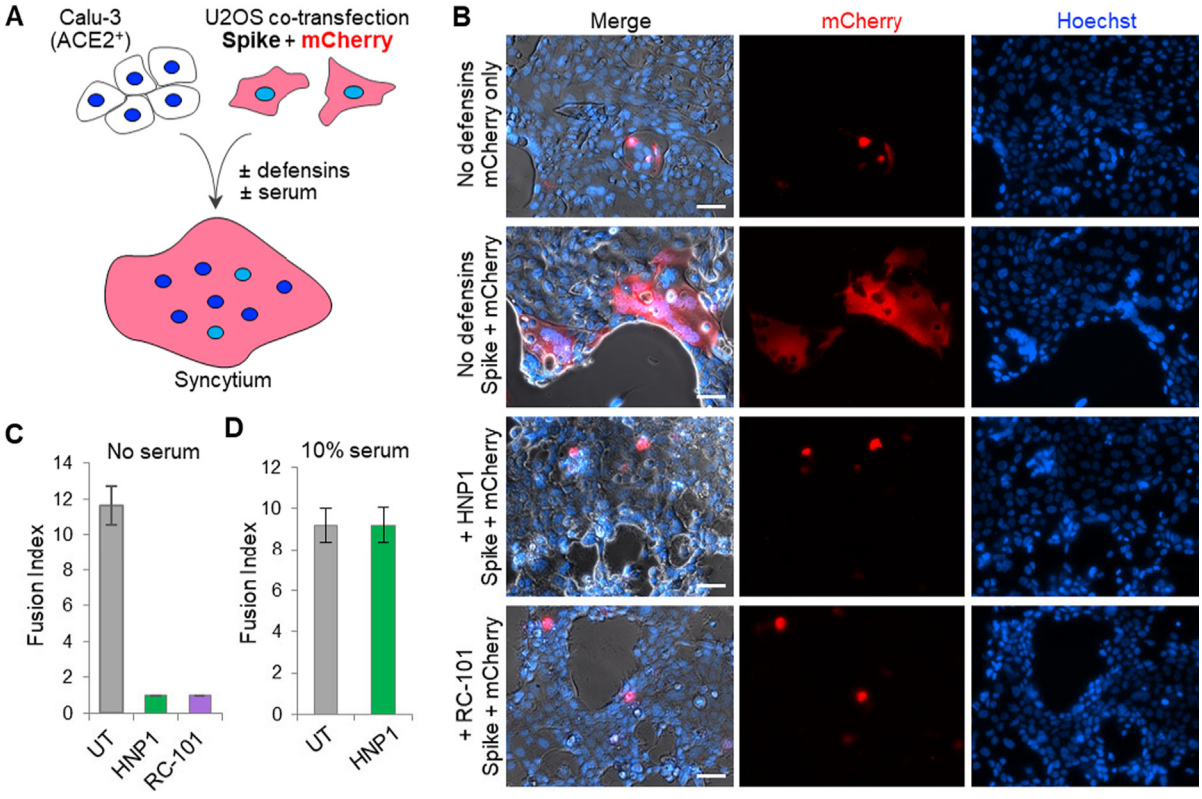

Figure 1. HNP1 and RC-101 inhibit SARS-CoV-2 Spike-mediated membrane fusion (A) A schematic of Spike-mediated syncytium formation assays. (B–D) U2OS cells co-transfected with SARS-CoV-2 Spike and mCherry were mixed with Calu-3 cells, co-cultured for 24 h in the absence or presence of 40 μM HNP1 or RC-101 and imaged by fluorescent microscopy to visualize mCherry and nuclei stained with Hoechst dye. (B) Representative images of the cells co-cultured in the absence of serum; scale bars are 50 μm. mCherry-positive cell syncytia were formed upon Spike expression in the absence of serum and defensins. (C, D) Fusion indices were quantified as an average number of nuclei per individual mCherry-positive syncytium (66–77 individual syncytia were quantified) in the absence (C) or presence of 10% serum (D). Data is presented as mean ± SE. UT – untreated cells without defensins.

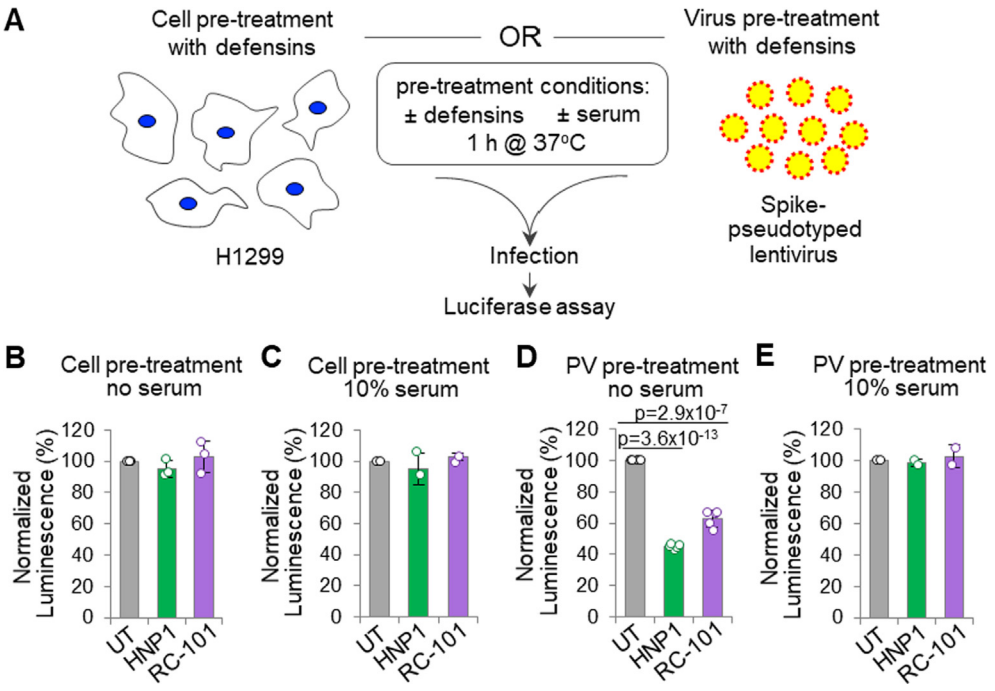

Figure 2. HNP1 and RC-101 inhibit SARS-CoV-2 Spike-pseudotyped viral infection (A) A schematic of Spike-pseudotyped lentiviral infection assays. (B–E) Infection efficiency of SARS-CoV-2 Spike-pseudotyped viruses encoding Nluc luciferase was monitored by luminescence assays. (B, C) H1299 cells were either untreated (UT) or pre-treated with 50 μM HNP1 or RC-101 before the addition of the pseudoviruses in the absence (n = 3; B) or presence of 10% serum (n = 2; C). (D, E) H1299 cells were transduced by pseudoviruses (PV), which were either untreated (UT) or pre-treated with 50 μM HNP1 or RC-101 before the addition to the cells in the absence (n = 3; D) or presence of 10% serum (n = 2; E). Data is presented as mean ± SE.

protein. Fluorescence anisotropy revealed that Cy5-HNP1 strongly binds to recombinant SARS-CoV-2 Spike with submicromolar affinity (K_d = 146 ± 18 nM; Figure 3(A)). Given the inhibitory effect of serum and the recognized role of serum proteins as defensin scavengers,[55] we measured whether Cy5-HNP1 can also bind serum albumin, the most abundant and highly interactive serum protein. Indeed, Cy5-HNP1 was able to bind to bovine serum albumin (BSA), but with over 20-fold lower affinity (K_d = 3.4 ± 0.3 μM; Figure 3(B)) as compared to Spike, indicating a much higher selectivity in binding the viral protein.

Defensins inactivate various structurally unrelated pathogen effector proteins such as bacterial toxins and viral proteins.[45,47,49] A common trait that unites these targets is their marginal thermodynamic stability dictated by the need for transitioning through dramatic conformational perturbations required for passing through narrow pores (i.e., for bacterial toxins) or fusing viral and host membranes (i.e., viral fusion proteins).[45,47,56] For viral proteins, conformational plasticity is also dictated by an ability of such proteins to tolerate high mutational loads, often needed for evading adaptive immune responses. SARS-CoV-2 Spike is subject to these evolutionary pressures and, as such, is anticipated to be prone to inactivation by defensins. Therefore, we assessed the effects of HNP1 and RC-101 on the stability of Spike using differential scanning fluorimetry (DSF).[57] Spike protein was destabilized at micromolar concentrations of HNP1 and RC-101 (Figure 3(C) and (D)) as implied from the impaired melting profile with a loss of the melting peak at its normal position and a higher signal at low temperatures (Figure 3(C)). Such behavior is characteristic of chemical denaturation[47] as it reports the fluorophore binding to hydrophobic residues of Spike exposed at temperatures below the original melting point of thermal denaturation. Since the signs of Spike destabilization by RC-101 were less prominent than for HNP1, we sought for additional experimental evidence confirming the mechanism of the inhibition.

Binding of HNP1 and RC-101 and locking of unfolded protein conformations can result in protein aggregation through exposed hydrophobic surfaces. Indeed, partial aggregation and precipitation of Spike was observed by pelleting upon incubation with HNP1 or RC-101 (Figure 3 (E)). These results imply that the dominant conformational state of Spike is compromised in the presence of defensins, which, therefore, are likely to interfere with its functional activity. Yet, given relatively mild destabilization and precipitation effects of RC-101, additional or

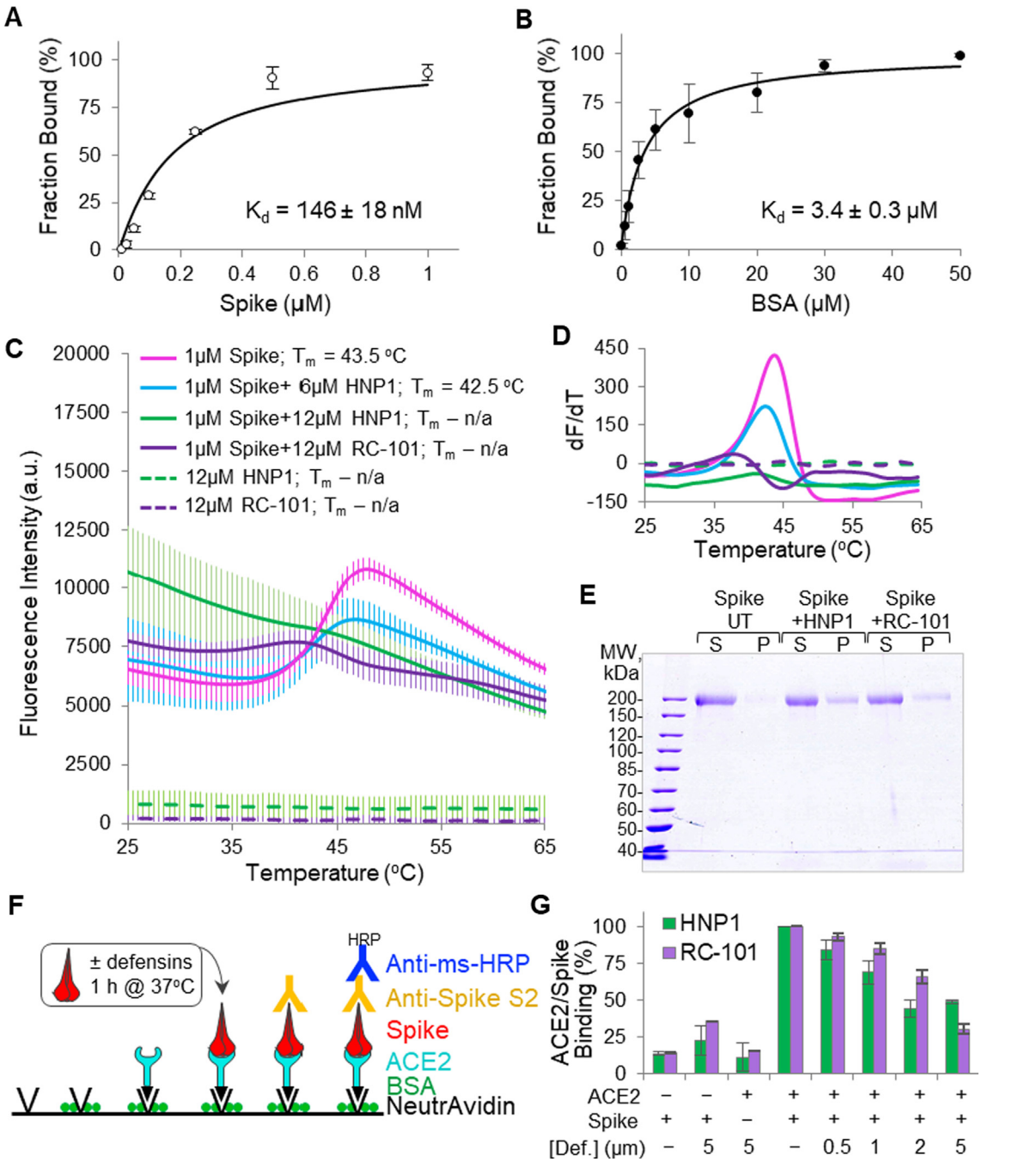

Figure 3. HNP1 and RC-101 destabilize SARS-CoV-2 Spike protein and inhibit its interaction with ACE2 (A, B) Binding of 50 nM Cy5-HNP1 to SARS-CoV-2 Spike (A) or BSA (B) was monitored by fluorescence anisotropy. Data from two independent experiments performed in duplicates is presented as mean ± SE. The K_ds were calculated by fitting the data to the binding isotherm equation (see Methods). The x-axis in (A) indicates the Spike monomer concentration. (C, D) Stability of SARS-CoV-2 Spike protein in the absence and presence of HNP1 and RC-101 was assessed by DSF. (C) Data from three independent DSF experiments is presented as mean ± SE. (D) First derivatives of the fluorescence versus time traces are shown. Melting temperatures (T_m) were calculated as the inflection points of the derivative curves; n/a – not applicable. (E) Precipitation of Spike by HNP1 and RC-101 was assessed by ultracentrifugation followed by SDS-PAGE of soluble (supernatant – S) and insoluble (pellet – P) fractions. (F) A schematic of Spike/ACE2 solid-phase binding assays. (G) Interaction of SARS-CoV-2 Spike with ACE2 in the absence and presence of HNP1 and RC-101 was tested in solid-phase binding assays. Data from three independent experiments is presented as mean ± SD. [Def.] is defensin concentration.

alternative mechanisms of Spike inhibition by defensins cannot be completely ruled out.

To test whether defensins can alter the Spike/ACE2 interaction, we developed a solid-phase binding assay (Figure 3(F)). We opted for surface attachment of biotinylated ACE2 on a NeutrAvidin-coated plate followed by blocking the plate with BSA. In this case, SARS-CoV-2 Spike could be pre-treated with defensins in the absence of BSA prior to addition to the ACE2-bound plate. To detect Spike protein bound to ACE2 we used anti-Spike S2 subunit antibody. In the absence of either ACE2 or Spike, the background signal was low, validating specificity of the assay (Figure 3 (G)). Higher background noise was detected in the presence of defensins at concentrations above 5 μM, which limited our ability to test the effects of higher doses of the peptides. Pre-incubation of Spike in the presence of HNP1 or RC-101 for 1 h at 37 °C inhibited Spike/ACE2 binding in a concentration-dependent manner (Figure 3(G)). Together our results demonstrate that defensins can bind SARS-CoV-2 Spike, alter its conformation, and impair its interaction with ACE2.

HNP1 and RC-101 inhibit SARS-CoV-2 infection

We next evaluated whether the inhibitory effects of HNP1 and RC-101 observed in the pseudovirus infections also occur when studying genuine SARS-CoV-2 infections in a BSL3-controlled environment. Vero E6 cells susceptible to SARS-CoV-2 infection[58] were infected with SARS-CoV-2, and the efficiency of infection was measured by flow cytometry staining for the viral nucleocapsid (N) protein. In the first set of experiments (Figure 4 (A)), the virus was pre-incubated with the defensins (50 μM final concentration) for 1 hour in the absence of serum. Under these conditions, SARS-CoV-2 infectivity was blocked by HNP1 and strongly inhibited by RC-101 (Figure 4(B) and (C)). Serum significantly reduced the ability of HNP1 to inhibit the infection in a concentration-dependent manner (Figure 4(D) and (E)). Next, we found that an hour-long pre-incubation is not required for the virus neutralization, as HNP1 and RC-101 inhibited SARS-CoV-2 infection when added to the cells immediately after the virus (Figure 5). Without serum, the inhibitory concentrations (IC_{50}) of HNP1 and RC-101 were 10.3 ± 0.9 and 29 ± 7.6 μM, respectively (Figure 5(D)–(G)). Notably, HNP1 strongly inhibited the SARS-CoV-2 infection even in the presence of 10% serum, providing that the peptide was present at sufficiently high concentration (e.g., 43 μM; Figure 5(B) and (C)).

Discussion

The data presented in this manuscript reveal that SARS-CoV-2 infection can be inhibited by two distinct defensins, and identify Spike as the target responsible for the observed inhibition. Defensins bound Spike with submicromolar affinities, promoted its unfolding and precipitation, and negatively affected interaction of Spike with ACE2, the receptor for SARS-CoV-2 entry into human cells. The quantitative difference in the efficiency of the defensin effects on SARS-CoV-2 vs pseudotyped lentiviral infection (notably more potent for authentic virus) in our study may be explained by several variables that differ in the experiments: the nature of parent viruses (SARS-CoV-2 vs HIV), cells (Vero E6 vs H1299), reporters (immunodetection of nucleocapsid followed by flow cytometry vs a luminescent reporter), and the level of serum (less controlled in the case of lentiviral assay due to technical reasons). The direct comparison of the K_d of HNP1 to Spike with the IC_{50} upon virus inhibition in cellular assays is similarly impractical due to several factors: the unknown stoichiometry of the inhibition, differences in solution and surface biochemistry, and the presence of other highly abundant binding partners of HNP1 (e.g., cell and virus membranes, to mention few) in the cellular assays.

While this manuscript was under revision, a complementary study was published that corroborates our main findings that α- and θ-defensins inhibit SARS-CoV-2 infection.[59] In agreement with our results, Xu and coauthors[59] found that HNP1 blocked Spike-mediated viral fusion; the inhibitory effects of defensins were more potent upon pre-incubation with the virus, in agreement with our conclusion that the inhibition is mediated by targeting viral rather than host molecules. These authors also attempted to assess the effects of defensins on Spike/ACE2 interactions using a solid-phase binding approach but failed to observe any inhibition, which may be due to a suboptimal experimental design. They chose to pre-treat ACE2 with defensins before its addition to immobilized Spike receptor-binding domain (RBD). Since ACE2 is an unlikely target of defensins, the overwhelming abundance of BSA (the ELISA blocking agent) over the target protein (Spike) upon addition of ACE2/defensin mixture to BSA/Spike-bound plate likely obscured the inhibitory effects detected in our study. Furthermore, supportive of the inhibitory effect of defensins on Spike/ACE2 interaction, Xu et al. reported that at 50 μg/ml (i.e., 14.5 μM final concentration) HNP1 significantly reduced the attachment of pseudotyped SARS-CoV-2 viruses to HeLa cells expressing ACE2. This concentration correlates with those used in our cellular assays (Figures 4 and 5), but is higher than those required to inhibit the interaction between Spike and ACE2 in the solid-phase assay (Figure 3(G)). This difference may reflect a distribution of defensins between additional targets present in cellular assays (*e.g.,* membranes, other proteins). Alternatively, higher doses

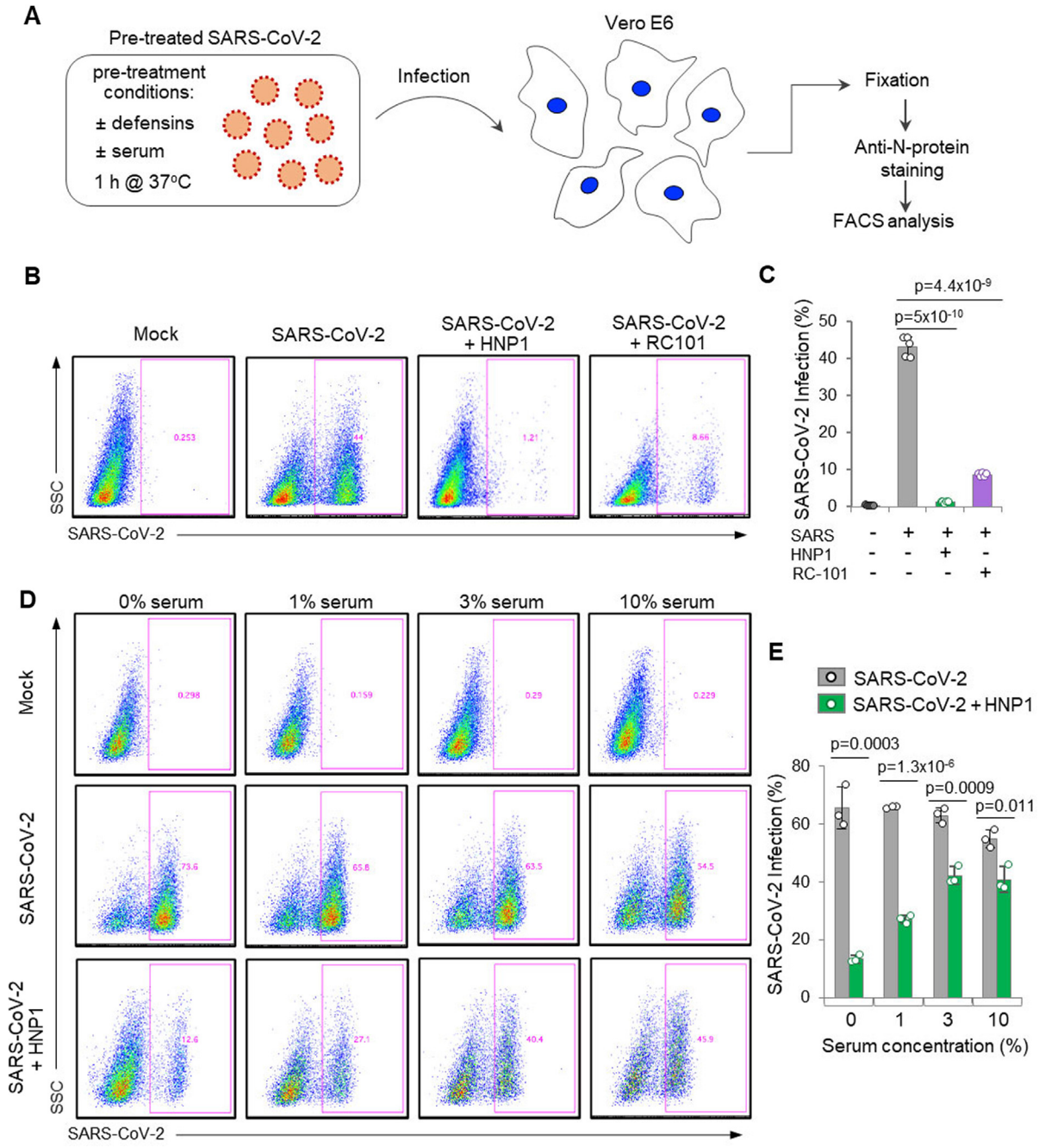

Figure 4. Pre-incubation of SARS-CoV-2 with defensins inhibits infection in a serum-dependent manner (A) A schematic of infection assays with defensin-pretreated SARS-CoV-2. (B,C) Cells were infected with the SARS-CoV-2 viruses pre-treated with 50 μM HNP1 or RC-101 in the absence of serum. (D, E) Cells were infected with the SARS-CoV-2 viruses pre-treated with 25 μM HNP1 with increasing serum concentrations. (B, D) Representative example flow cytometry plots are shown for each condition. (C, E) Graphs depict mean infection percentage measurements from experiments conducted in 5 or 3 replications. Error bars represent the SD of the mean.

of defensins may be required to overcome the avidity of the highly multimeric cell-virus interaction. Of note, since the recombinant Spike protein used in our *in vitro* assays was stabilized in the prefusion conformation by mutations (K986P and V987P), the destabilizing effects of defensins on native Spike might be even more prominent.

Although destabilization of Spike by defensins, resulting in its compromised interaction with ACE2, is a likely mechanism behind the inhibition of SARS-CoV-2 infection of human cells, we recognize that the effects of defensins on viruses are multifaceted[18] and may extend beyond the inhibition of Spike/ACE2 interaction reported here. Due

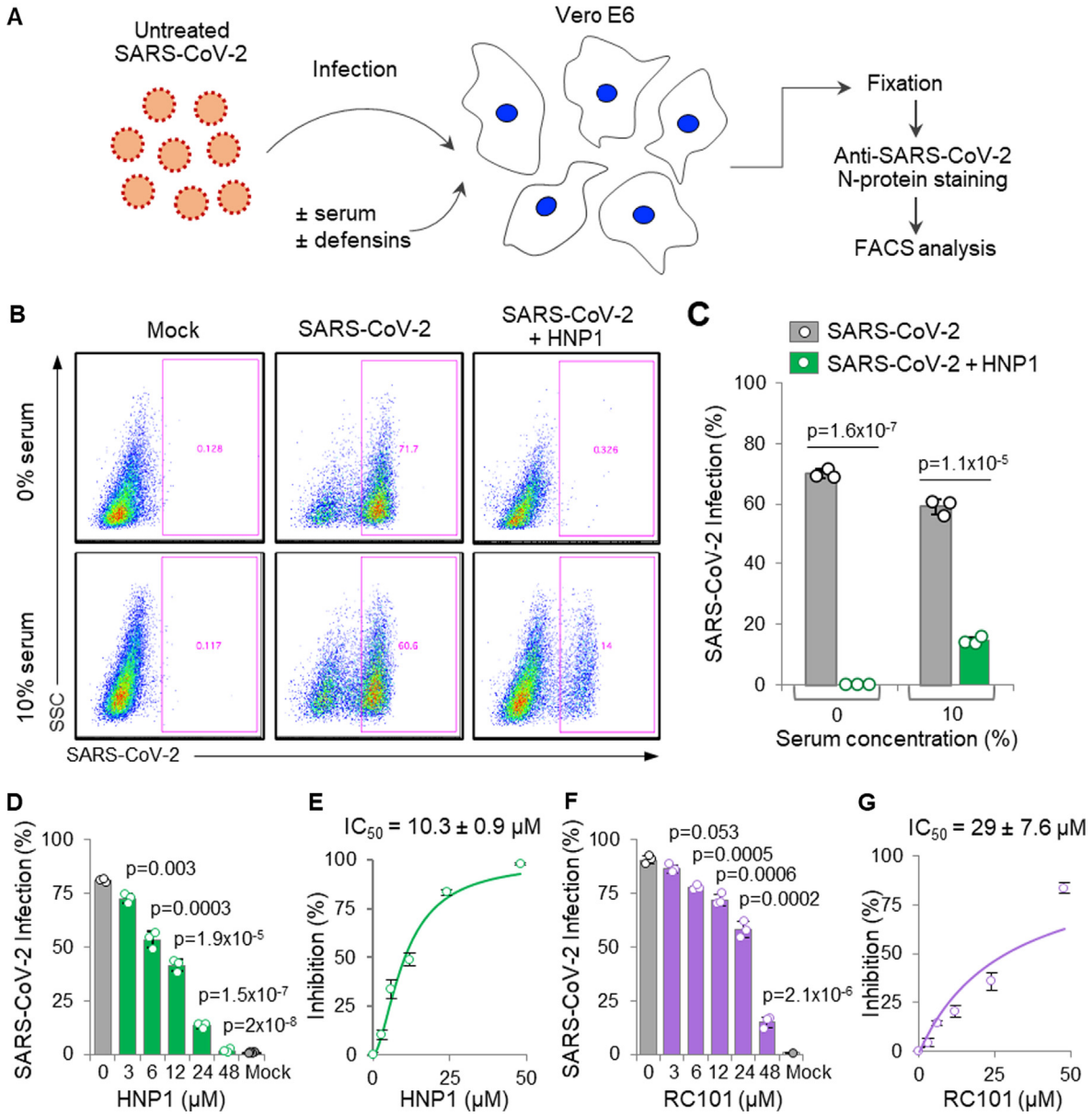

Figure 5. HNP1 and RC-101 inhibit SARS-CoV-2 infection without virus pre-incubation (A) A schematic of SARS-CoV-2 infection assays. Defensins were added at the time of infection without pre-incubation with the virus. (B, C) Cells were infected with SARS-CoV-2 in the presence of 43 μM HNP1 in the absence and presence of 10% serum. (D–G) Cells were infected with SARS-CoV-2 in the absence of serum with increasing concentrations of HNP1 (D, E) or RC-101 (E, F) to calculate IC_{50} (E, G) by fitting the data from (D, F) to the Hill's equation (see Methods). All experiments were conducted in three replications. Error bars represent the SD of the mean.

to the broad nature of defensin interactions with affected proteins, other mechanisms (e.g., blocking protease cleavage, or preventing conformational changes needed for fusion) may contribute to the inhibition of Spike by defensins. Although destabilization, as reflected in lower melting temperatures, is the extreme manifestation of the defensins on target proteins, lower doses of defensins likely cause less-notable perturbations to the protein structure, which can, nevertheless, be functionally consequential. Most importantly, the pliable, metastable nature of viral proteins is a primary reason for their higher susceptibility to the effects of defensins compared to most host proteins. The ability of defensins to get integrated into the hydrophobic core of such proteins defines the unusual combination of a broad specificity and high affinity of these interactions.

In our study, the ability of α-, and θ-defensins to promote unfolding of pathogenic proteins[45] is confirmed on a yet another viral pathogen. We propose that this ability plays a key role in various aspects of the protective mechanisms employed by defensins

when viral proteins are involved. Perhaps counterintuitively, even the reported stabilization of viral capsids by defensins[60] may result from prior unfolding by defensins of conformationally pliable regions at the capsid protein interface with their subsequent engagement in abnormal hydrophobic interactions resistant to the changes required for programmed capsid disassembly. The resulting effect of capsid stabilization may be likened to melting required for soldering metal surfaces or bonding plastic surfaces via their prior solubilization.

We found that micromolar concentrations of α-defensin HNP1 and θ-defensin (retrocyclin) RC-101 are capable of inhibiting SARS-CoV-2 infection *in vitro*. In comparison, levels of α-defensins detected in body liquids are typically lower than what is required for robust virus inhibition. For example, the level of HNP1-4 in the nasal aspirates of children affected by adenovirus is about 220 ng/mL (∼0.07 μM).[61] In peripheral blood of COVID-19 patients, the levels of HNP1-3 vary from ∼ 1.5 to 7.6 nM.[62] However, these low levels can be misleading given that HNP1-4 defensins are produced by neutrophils, whose effects are typically restricted to local environments where they are most needed. Indeed, higher local levels of HNP1-4 than those needed for inhibition of SARS-CoV-2 are expected near neutrophils before dilution by body fluids.[63] Furthermore, the highly interactive, "sticky" nature of defensins and their ability to cause precipitation of partner proteins is another factor contributing to higher local and lower systemic levels of defensins.

Therapeutic application of defensins and other antimicrobial peptides as antiviral agents has been suggested.[64,65] Since the inhibitory effects of the HNP1 and RC-101 against SARS-CoV-2 are diminished by serum, the defensins perhaps can be most effective as topical antiviral agents (e.g., intranasal). Similarly, retrocyclins have been proposed as topical microbicides to prevent sexually transmitted infections caused by HIV-1.[66,67] Notably, owing to their cyclic nature, high stability, and resistance to proteolysis, retrocyclins are particularly promising as therapeutic agents. Retrocyclins have low toxicity in cell cultures and *in vivo*, are well tolerated in animal models, and are non-immunogenic in chimpanzees.[68,69] Together our data suggest that HNP1 and RC-101 should be further evaluated as candidates for developing topical anti-COVID-19 and broad-range antiviral drugs.

Materials and Methods

Peptides, proteins, and DNA constructs

HNP1 and RC-101 were prepared by solid-phase peptide synthesis, and the correct folding was ensured as described previously.[70–73] The activity of HNP1 and RC-101 was confirmed using the recombinant actin cross-linking domain (ACD) of *Vibrio cholerae* MARTX toxin.[47]

Recombinant His-tagged biotinylated ACE2 (#BT933-020) and recombinant HEK293-derived full-length His-tagged SARS-CoV-2 Spike glycoprotein (#10549-CV) were purchased from R&D Systems (Minneapolis, MN). The recombinant Spike protein (V16-K1211 with a C-term His tag) contains two stabilizing mutations, K986P and V987P, to promote the prefusion conformation, and two mutations, R682S and R685S, eliminating a furin protease cleavage site. According to the manufacturer's QC data, Spike protein is active and displays consistent, high-affinity binding to ACE2 (K_d = 1.72 nM determined by SPR) in ELISA tests and to ACE2-expressing cells in functional flow cytometry tests. Bovine serum albumin (BSA) was purchased from ThermoFisher Scientific (Waltham, MA).

pCAGGS vector encoding SARS-CoV-2 Spike glycoprotein was obtained from BEI Resources (Manassas, VA; deposited by Dr. Florian Krammer, Icahn School of Medicine at Mount Sinai). Lentiviral NanoLuc expression vector (a gift from Erich Wanker; Addgene plasmid #113450; RRID:Addgene_113450[74] was modified to introduce IL6 secretion signal (IL6ss) upstream of Myc-Nluc using PCR-based approach with NEBuilder DNA assembly (New England Biolabs, Ipswich, MA). Lentiviral helper plasmids expressing HIV Gag-Pol, HIV Tat, or HIV Rev under a CMV promoter were obtained from BEI Resources (Manassas, VA; deposited by Dr. Jesse Bloom, Fred Hutchinson Cancer Research Center).

Cell lines

All cells were cultured at 37 °C with 5% CO_2 in a humidified incubator. U2OS and Vero E6 cells were grown in Dulbecco's Modified Eagle Medium, H1299 – in RPMI-1640 medium, Calu-3 – in Eagle's Minimum Essential Medium, all supplemented with 1% penicillin–streptomycin and 10% fetal bovine serum (FBS). H1299, Calu-3, Vero E6, and HEK293T cells were purchased from ATCC. The identity and purity of the U2OS cells were verified by STR profiling (Amelogenin + 9 loci) at the Genomic Shared Resource (OSU, Comprehensive Cancer Center) with 100% match using The Cellosaurus cell line database.[75] All cell lines were mycoplasma-negative as determined by a PCR-based approach.[76]

Spike-mediated cell fusion assays

Using Lipofectamine 3000 reagent (Thermo Fisher Scientific, Waltham, MA), U2OS cells were co-transfected with pmCherry and pCAGGS vector encoding SARS-CoV-2 Spike protein. For a negative control, U2OS cells were transfected with pmCherry only. 24-hours post-transfection, U2OS cells were trypsinized, mixed with Calu-3 cells on 96-well μ-plate (Ibidi, Germany), and incubated for

24 h in the presence (40 μM; final concentration) or absence of HNP1 or RC-101, with (10%; final concentration) or without FBS. Following the incubation, the co-cultures were counterstained with 1 μg/mL Hoechst 33342 (Invitrogen, Carlsbad, CA) and imaged using Nikon inverted microscope Eclipse Ti-E (Nikon Instruments, Melville, NY). Nikon NIS Elements AR software was used to quantify fusion indices calculated as number of nuclei per individual mCherry-positive syncytium.

Fluorescence anisotropy

Increasing concentrations of SARS-CoV-2 Spike protein or BSA were incubated with 50 nM Cy5-labeled HNP1 in phosphate buffered saline (PBS). Fluorescence anisotropy was measured using a Tecan Infinite M1000Pro plate reader (Tecan SP, Inc., Baldwin Park, CA). K_d values were determined by fitting the experimental data to the binding isotherm equation:

$$Fraction\ S\ Bound = \frac{S + D + K_d - \sqrt{(S + D + K_d)^2 - 4 * S * D}}{2 * D}$$

where S is the concentration of Spike (or BSA) and D is the concentration of defensin (Cy5-HNP1).

Differential scanning fluorimetry (DSF)

DSF was performed as described previously.[47,56] Briefly, SARS-CoV-2 Spike protein was diluted to 1 μM (calculated as monomer concentration) in PBS in the absence or presence of HNP1 or RC-101 and supplemented with 1:5000 dilution of Sypro Orange dye (Invitrogen, Carlsbad, CA). Changes in fluorescence of the dye, which preferentially binds to protein hydrophobic regions exposed upon thermal-induced unfolding, were measured using a CFX real-time PCR detection system (Bio-Rad, Hercules, CA). The melting temperatures (T_m) were determined as the maximum of the first derivative (dF/dT) of each normalized experimental curve.

SARS-CoV-2 spike protein precipitation assays

To assess protein precipitation, 1 μM of Spike protein (calculated as monomer concentration; R&D Systems #10549-CV) in PBS was incubated in the absence or presence of 12 μM HNP1 or RC-101 for 30 min at 37 °C followed by centrifugation at 100,000*g* for 30 min at 37 °C using TLA-100 rotor in Optima MAX-TL ultracentrifuge (Beckman Coulter, Brea, CA). Supernatant factions containing soluble protein were carefully collected without disturbing the pellets and supplemented with 4x reducing sample buffer. Pellets containing precipitated insoluble protein were soaked and resuspended in 1x reducing sample buffer prepared from the 4x concentrate by diluting in PBS. The resulting volumes of pellet fractions were kept equal to the supernatant volumes. All samples were boiled for 5 min and equal amounts were loaded and resolved on SDS-PAGE.

Solid-phase ACE2/Spike binding assays

High-binding 384-well plates (Greiner-Bio-One #781061) were coated with 25 μL per well of 5 μg/mL NeutrAvidin (ThemoFisher Scientific #31000) in 50 mM sodium carbonate buffer, pH 9.4 for 8 h at 37 °C. Unbound NeutrAvidin was removed by washing three times with 50 μL per well of PBS supplemented with 0.05% Tween-20 (all subsequent washing steps were done similarly). The wells were blocked overnight at room temperature with 50 μL per well of 5% BSA in PBS. Following washing, 2 μg/mL of biotinylated ACE2 (R&D Systems #BT933-020) in PBS was loaded (25 μL per well) and incubated for 1 h at 37 °C. At the same time, SARS-CoV-2 Spike protein (R&D Systems #10549-CV) was pre-incubated in the absence and presence of defensins for 1 h at 37 °C. Unbound ACE2 was washed out and 25 μL per well of the pre-incubated Spike was loaded and allowed to bind for 1 h at 37 °C. Following washing, the plate was incubated with mouse anti-Spike antibody detecting SARS-CoV-2 Spike S2 subunit (R&D Systems #MAB10557; 1:2000) for 30 min at 37 °C, followed by incubation with anti-mouse antibody conjugated with horsereddish peroxidase (HRP; Sigma #A4416; 1:10000). The signal was developed using a colorimetric HRP substrate tetramethylbenzidine (TMB; ThemoFisher Scientific), stopped by 1 N hydrochloric acid, and the absorbance was recorder by a Tecan Infinite M1000Pro plate reader at 450 nm. The data was normalized to a negative control (no-ACE2/no-Spike) set as zero and the readings from the ACE2 wells incubated with Spike in the absence of defensins set as 100%. Additional controls included Spike-treated wells with and without pre-incubation with defensins in the absence of ACE2.

Pseudotyped virus production, cell infection, and luciferase assays

Virus-like particles pseudotyped with SARS-CoV-2 Spike protein were produced by transfecting HEK293T cells with pLenti-IL6ss-Myc-Nluc, pCAGGS-SARS-CoV-2 Spike plasmid, HIV Gag-Pol plasmid, HIV Tat plasmid, and HIV Rev plasmid using Fugene 6 transfection reagent (Promega, Madison, WI). Virus-containing medium was titrated to ensure undersaturating conditions for infection of H1299 cells. H1299 cells were incubated with the pseudovirus for 24 h followed by luciferase assays performed using NanoGlo Luciferase Assay System (Promega, Madison,

WI). In one set of experiments, H1299 cells were pre-treated with the defensins in the absence or presence of 10% serum before the addition of the pseudovirus; in the other set of exepriments, pseudovirus was pre-incubated with 50 μM defensins prior to addition to cells. Luminescence signals were recorded using a Tecan Infinite M1000Pro plate reader (Tecan SP, Inc., Baldwin Park, CA).

SARS-CoV-2 infections and flow cytometry

SARS-CoV-2 strain USA-WA1/2020 provided by BEI Resources was plaque purified on Vero E6 cells to identify plaques lacking mutations in the Spike protein furin cleavage site. Non-mutated plaques were then propagated using Vero E6 cells stably expressing TMPRSS2 (kindly provided by Dr. Shan-Lu Liu, Ohio State University). Virus-containing supernatant aliquots were snap frozen in liquid nitrogen and stored at −80 °C. The virus stock was titered on Vero E6 cells. For infection experiments, virus at an MOI of 1 was used to infect Vero E6 in the presence or absence of FBS or defensins. For the virus pre-treatment experiments, SARS-CoV-2 was pre-incubated with the defensins for 1 h at 37 °C before the addition to the cells (Figure 4(A)). For the experiments without virus/defensin pre-incubation, virus and defensins were added to the cells immediately one after the other without the initial pre-incubation (Figure 5(A)). After 24 h, cells were trypsinized, fixed with 4% paraformaldehyde for 1 h at room temperature, permeabilized with 0.1% Triton X100 in PBS, and stained with anti-SARS-CoV-2 N protein antibody (Sino Biological, Wayne, PA; #40143-MM08). Primary antibody labeling was followed by goat anti-mouse Alexa Fluor 647 secondary antibody (Life Technologies, Carlsbad, CA). Flow cytometry data acquisition was performed using a FACSCanto II flow cytometer (BD Biosciences, San Jose, CA). Data was analyzed using FlowJo software. Mock infected control samples were used to set gates for quantification of infected cell percentages.

Inhibitory concentration (IC_{50}) of HNP1 and RC-101 was determined by fitting the data to the Hill equation:

$$\%Inhibiton = (I_{max} * D^n)/(IC_{50}{}^n + D^n)$$

where I_{max} is the maximal inhibition, D is the concentration of defensin, n is the Hill coefficient.

Statistical analysis

Data are presented as mean values from several independent experiments (as indicated in the figure legends); error bars represent standard deviations (SD) or standard errors (SE) of the mean. ANOVA followed by multiple comparison tests with Bonferroni correction was applied using the Analysis ToolPak (a Microsoft Excel add-in program); individual p-values are indicated on the graph figures.

Funding

This work was supported by COVID-19 Seed Grants from the Office of Research of The Ohio State University (to DSK, AS, and JSY), National Natural Science Foundation of China #82030062 (to WL), NIH R01 grants: GM114666 (to DSK), AI130110, AI151230, and HL154001 (to JSY), and NIH R00 AI125136 (to AS). The content is solely the responsibility of the authors and does not necessarily represent the official views of the National Institutes of Health.

CRediT authorship contribution statement

Elena Kudryashova: Conceptualization, Methodology, Validation, Formal analysis, Investigation, Writing – original draft, Writing – review & editing, Visualization. **Ashley Zani:** Investigation, Writing – review & editing. **Geraldine Vilmen:** Investigation, Writing – review & editing. **Amit Sharma:** Conceptualization, Validation, Writing – review & editing, Supervision, Funding acquisition. **Wuyuan Lu:** Resources, Writing – review & editing. **Jacob S. Yount:** Formal analysis, Resources, Writing – review & editing, Supervision, Project administration, Funding acquisition. **Dmitri S. Kudryashov:** Conceptualization, Methodology, Validation, Resources, Writing – original draft, Writing – review & editing, Supervision, Project administration, Funding acquisition.

DECLARATION OF COMPETING INTEREST

The authors declare that they have no known competing financial interests or personal relationships that could have appeared to influence the work reported in this paper.

Received 28 May 2021;
Accepted 27 August 2021;
Available online xxxx

Keywords:
SARS-CoV-2;
innate immunity;
defensins;
human neutrophil peptide HNP1;
retrocyclin RC-101

References

1. Ksiazek, T.G., Erdman, D., Goldsmith, C.S., Zaki, S.R., Peret, T., Emery, S., et al., (2003). A novel coronavirus

associated with severe acute respiratory syndrome. *N. Engl. J. Med.*, **348**, 1953–1966.
2. Novel Swine-Origin Influenza, A.V.I.T., Dawood, F.S., Jain, S., Finelli, L., Shaw, M.W., Lindstrom, S., et al., (2009). Emergence of a novel swine-origin influenza A (H1N1) virus in humans. *N. Engl. J. Med.*, **360**, 2605–2615.
3. Lu, G., Liu, D., (2012). SARS-like virus in the Middle East: a truly bat-related coronavirus causing human diseases. *Protein Cell.*, **3**, 803–805.
4. Petersen, E., Koopmans, M., Go, U., Hamer, D.H., Petrosillo, N., Castelli, F., et al., (2020). Comparing SARS-CoV-2 with SARS-CoV and influenza pandemics. *Lancet Infect. Dis.*, **20**, e238–e244.
5. Mizumoto, K., Kagaya, K., Zarebski, A., Chowell, G., (2020). Estimating the asymptomatic proportion of coronavirus disease 2019 (COVID-19) cases on board the Diamond Princess cruise ship, Yokohama, Japan, 2020. *Euro. Surveill.*, **25**
6. Nishiura, H., Kobayashi, T., Miyama, T., Suzuki, A., Jung, S.M., Hayashi, K., et al., (2020). Estimation of the asymptomatic ratio of novel coronavirus infections (COVID-19). *Int. J. Infect. Dis.*, **94**, 154–155.
7. Oran, D.P., Topol, E.J., (2020). Prevalence of asymptomatic SARS-CoV-2 infection: a narrative review. *Ann. Intern. Med.*, **173**, 362–367.
8. Park, A., Iwasaki, A., (2020). Type I and Type III interferons - induction, signaling, evasion, and application to combat COVID-19. *Cell Host Microbe*, **27**, 870–878.
9. Peacock, T.P., Goldhill, D.H., Zhou, J., Baillon, L., Frise, R., Swann, O.C., et al., (2021). The furin cleavage site in the SARS-CoV-2 spike protein is required for transmission in ferrets. *Nature Microbiol.*, **6**, 899–909.
10. Shi, G., Kenney, A.D., Kudryashova, E., Zani, A., Zhang, L., Lai, K.K., et al., (2021). Opposing activities of IFITM proteins in SARS-CoV-2 infection. *EMBO J.*, **40**, e106501
11. Winstone, H., Lista, M.J., Reid, A.C., Bouton, C., Pickering, S., Galao, R.P., et al., (2021). The polybasic cleavage site in SARS-CoV-2 spike modulates viral sensitivity to type I interferon and IFITM2. *J. Virol.*, **95**
12. Nchioua, R., Kmiec, D., Muller, J.A., Conzelmann, C., Gross, R., Swanson, C.M., et al., (2020). SARS-CoV-2 Is restricted by zinc finger antiviral protein despite preadaptation to the low-CpG environment in humans. *mBio*, **11**
13. Pfaender, S., Mar, K.B., Michailidis, E., Kratzel, A., Boys, I. N., V'Kovski, P., et al., (2020). LY6E impairs coronavirus fusion and confers immune control of viral disease. *Nature Microbiol.*, **5**, 1330–1339.
14. Wang, S., Li, W., Hui, H., Tiwari, S.K., Zhang, Q., Croker, B.A., et al., (2020). Cholesterol 25-Hydroxylase inhibits SARS-CoV-2 and other coronaviruses by depleting membrane cholesterol. *EMBO J.*, **39**, e106057
15. Zang, R., Case, J.B., Yutuc, E., Ma, X., Shen, S., Gomez Castro, M.F., et al., (2020). Cholesterol 25-hydroxylase suppresses SARS-CoV-2 replication by blocking membrane fusion. *Proc. Natl. Acad. Sci. USA*, **117**, 32105–32113.
16. Zhao, X., Zheng, S., Chen, D., Zheng, M., Li, X., Li, G., et al., (2020). LY6E restricts entry of human coronaviruses, including currently pandemic SARS-CoV-2. *J. Virol.*, **94**
17. Brice, D.C., Diamond, G., (2020). Antiviral activities of human host defense peptides. *Curr. Med. Chem.*, **27**, 1420–1443.
18. Holly, M.K., Diaz, K., Smith, J.G., (2017). Defensins in viral infection and pathogenesis. *Annu. Rev. Virol.*, **4**, 369–391.
19. Klotman, M.E., Chang, T.L., (2006). Defensins in innate antiviral immunity. *Nature Rev. Immunol.*, **6**, 447–456.
20. Wohlford-Lenane, C.L., Meyerholz, D.K., Perlman, S., Zhou, H., Tran, D., Selsted, M.E., et al., (2009). Rhesus theta-defensin prevents death in a mouse model of severe acute respiratory syndrome coronavirus pulmonary disease. *J. Virol.*, **83**, 11385–11390.
21. Ganz, T., (2003). Defensins: antimicrobial peptides of innate immunity. *Nature Rev. Immunol.*, **3**, 710–720.
22. Lehrer, R.I., (2004). Primate defensins. *Nature Rev. Microbiol.*, **2**, 727–738.
23. Selsted, M.E., Ouellette, A.J., (2005). Mammalian defensins in the antimicrobial immune response. *Nature Immunol.*, **6**, 551–557.
24. Zasloff, M., (2002). Antimicrobial peptides of multicellular organisms. *Nature*, **415**, 389–395.
25. Zasloff, M., (2019). Antimicrobial peptides of multicellular organisms: my perspective. *Adv. Exp. Med. Biol.*, **1117**, 3–6.
26. Tang, Y.Q., Yuan, J., Osapay, G., Osapay, K., Tran, D., Miller, C.J., et al., (1999). A cyclic antimicrobial peptide produced in primate leukocytes by the ligation of two truncated alpha-defensins. *Science*, **286**, 498–502.
27. Lehrer, R.I., Cole, A.M., Selsted, M.E., (2012). theta-Defensins: cyclic peptides with endless potential. *J. Biol. Chem.*, **287**, 27014–27019.
28. Venkataraman, N., Cole, A.L., Ruchala, P., Waring, A.J., Lehrer, R.I., Stuchlik, O., et al., (2009). Reawakening retrocyclins: ancestral human defensins active against HIV-1. *PLoS Biol.*, **7**, e95
29. Cole, A.M., Hong, T., Boo, L.M., Nguyen, T., Zhao, C., Bristol, G., et al., (2002). Retrocyclin: a primate peptide that protects cells from infection by T- and M-tropic strains of HIV-1. *Proc. Natl. Acad. Sci. USA*, **99**, 1813–1818.
30. Tran, D., Tran, P.A., Tang, Y.Q., Yuan, J., Cole, T., Selsted, M.E., (2002). Homodimeric theta-defensins from rhesus macaque leukocytes: isolation, synthesis, antimicrobial activities, and bacterial binding properties of the cyclic peptides. *J. Biol. Chem.*, **277**, 3079–3084.
31. Yasin, B., Wang, W., Pang, M., Cheshenko, N., Hong, T., Waring, A.J., et al., (2004). Theta defensins protect cells from infection by herpes simplex virus by inhibiting viral adhesion and entry. *J. Virol.*, **78**, 5147–5156.
32. Cole, A.M., Patton, D.L., Rohan, L.C., Cole, A.L., Cosgrove-Sweeney, Y., Rogers, N.A., et al., (2010). The formulated microbicide RC-101 was safe and antivirally active following intravaginal application in pigtailed macaques. *PLoS ONE*, **5**, e15111
33. Sassi, A.B., Bunge, K.E., Hood, B.L., Conrads, T.P., Cole, A.M., Gupta, P., et al., (2011). Preformulation and stability in biological fluids of the retrocyclin RC-101, a potential anti-HIV topical microbicide. *AIDS Res. Ther.*, **8**, 27.
34. Sassi, A.B., Cost, M.R., Cole, A.L., Cole, A.M., Patton, D. L., Gupta, P., et al., (2011). Formulation development of retrocyclin 1 analog RC-101 as an anti-HIV vaginal microbicide product. *Antimicrob. Agents Chemother.*, **55**, 2282–2289.
35. Lehrer, R.I., Lu, W., (2012). alpha-Defensins in human innate immunity. *Immunol. Rev.*, **245**, 84–112.
36. Harwig, S.S., Park, A.S., Lehrer, R.I., (1992). Characterization of defensin precursors in mature human neutrophils. *Blood*, **79**, 1532–1537.
37. de Leeuw, E., Li, C., Zeng, P., Li, C., Diepeveen-de Buin, M., Lu, W.Y., et al., (2010). Functional interaction of human

neutrophil peptide-1 with the cell wall precursor lipid II. *FEBS Letters*, **584**, 1543–1548.
38. Ericksen, B., Wu, Z., Lu, W., Lehrer, R.I., (2005). Antibacterial activity and specificity of the six human {alpha}-defensins. *Antimicrob. Agents Chemother.*, **49**, 269–275.
39. Lehrer, R.I., Barton, A., Daher, K.A., Harwig, S.S., Ganz, T., Selsted, M.E., (1989). Interaction of human defensins with Escherichia coli. Mechanism of bactericidal activity. *J. Clin. Invest.*, **84**, 553–561.
40. Varkey, J., Nagaraj, R., (2005). Antibacterial activity of human neutrophil defensin HNP-1 analogs without cysteines. *Antimicrob. Agents Chemother.*, **49**, 4561–4566.
41. Edgerton, M., Koshlukova, S.E., Araujo, M.W., Patel, R.C., Dong, J., Bruenn, J.A., (2000). Salivary histatin 5 and human neutrophil defensin 1 kill Candida albicans via shared pathways. *Antimicrob. Agents Chemother.*, **44**, 3310–3316.
42. Lehrer, R.I., Ganz, T., Szklarek, D., Selsted, M.E., (1988). Modulation of the in vitro candidacidal activity of human neutrophil defensins by target cell metabolism and divalent cations. *J. Clin. Invest.*, **81**, 1829–1835.
43. Ding, J., Chou, Y.Y., Chang, T.L., (2009). Defensins in viral infections. *J. Innate Immun.*, **1**, 413–420.
44. Wilson, S.S., Wiens, M.E., Smith, J.G., (2013). Antiviral mechanisms of human defensins. *J. Mol. Biol.*, **425**, 4965–4980.
45. Kudryashova, E., Koneru, P.C., Kvaratskhelia, M., Stromstedt, A.A., Lu, W., Kudryashov, D.S., (2016). Thermodynamic instability of viral proteins is a pathogen-associated molecular pattern targeted by human defensins. *Sci. Rep.*, **6**, 32499.
46. Kudryashova, E., Lu, W., Kudryashov, D.S., (2015). Defensins versus pathogens: an unfolding story. *Oncotarget.*, **6**, 28533–28534.
47. Kudryashova, E., Quintyn, R., Seveau, S., Lu, W., Wysocki, V.H., Kudryashov, D.S., (2014). Human defensins facilitate local unfolding of thermodynamically unstable regions of bacterial protein toxins. *Immunity*, **41**, 709–721.
48. Kudryashova, E., Seveau, S.M., Kudryashov, D.S., (2017). Targeting and inactivation of bacterial toxins by human defensins. *Biol. Chem.*, **398**, 1069–1085.
49. Kudryashova, E., Seveau, S., Lu, W., Kudryashov, D.S., (2015). Retrocyclins neutralize bacterial toxins by potentiating their unfolding. *Biochem. J.*, **467**, 311–320.
50. Wang, C., Wang, S., Li, D., Wei, D.Q., Zhao, J., Wang, J., (2020). Human intestinal defensin 5 inhibits SARS-CoV-2 invasion by cloaking ACE2. *Gastroenterology*, **159** 1145–7 e4.
51. Ou, X., Liu, Y., Lei, X., Li, P., Mi, D., Ren, L., et al., (2020). Characterization of spike glycoprotein of SARS-CoV-2 on virus entry and its immune cross-reactivity with SARS-CoV. *Nature Commun.*, **11**, 1620.
52. Buchrieser, J., Dufloo, J., Hubert, M., Monel, B., Planas, D., Rajah, M.M., et al., (2020). Syncytia formation by SARS-CoV-2-infected cells. *EMBO J.*, **39**, e106267
53. Chang, T.L., Vargas Jr., J., DelPortillo, A., Klotman, M.E., (2005). Dual role of alpha-defensin-1 in anti-HIV-1 innate immunity. *J. Clin. Invest.*, **115**, 765–773.
54. Demirkhanyan, L.H., Marin, M., Padilla-Parra, S., Zhan, C., Miyauchi, K., Jean-Baptiste, M., et al., (2012). Multifaceted mechanisms of HIV-1 entry inhibition by human alpha-defensin. *J. Biol. Chem.*, **287**, 28821–28838.
55. Panyutich, A., Ganz, T., (1991). Activated alpha 2-macroglobulin is a principal defensin-binding protein. *Am. J. Respir. Cell Mol. Biol.*, **5**, 101–106.
56. Kudryashova, E., Heisler, D., Zywiec, A., Kudryashov, D. S., (2014). Thermodynamic properties of the effector domains of MARTX toxins suggest their unfolding for translocation across the host membrane. *Mol. Microbiol.*, **92**, 1056–1071.
57. Niesen, F.H., Berglund, H., Vedadi, M., (2007). The use of differential scanning fluorimetry to detect ligand interactions that promote protein stability. *Nature Protoc.*, **2**, 2212–2221.
58. Chu, H., Chan, J.F., Yuen, T.T., Shuai, H., Yuan, S., Wang, Y., et al., (2020). Comparative tropism, replication kinetics, and cell damage profiling of SARS-CoV-2 and SARS-CoV with implications for clinical manifestations, transmissibility, and laboratory studies of COVID-19: an observational study. *Lancet Microbe*, **1**, e14–e23.
59. Xu, C., Wang, A., Marin, M., Honnen, W., Ramasamy, S., Porter, E., et al., (2021). Human defensins inhibit SARS-CoV-2 infection by blocking viral entry. *Viruses*, **13**
60. Gulati, N.M., Miyagi, M., Wiens, M.E., Smith, J.G., Stewart, P.L., (2019). alpha-defensin HD5 stabilizes human papillomavirus 16 capsid/core interactions. *Pathog Immun.*, **4**, 196–234.
61. Priyadharshini, V.S., Ramirez-Jimenez, F., Molina-Macip, M., Renteria-Rosales, C., Santiago-Cruz, J., Zarate-Segura, P., et al., (2018). Human neutrophil defensin-1, -3, and -4 are elevated in nasal aspirates from children with naturally occurring adenovirus infection. *Can. Respir. J.*, **2018**, 1038593.
62. Abdeen, S., Bdeir, K., Abu-Fanne, R., Maraga, E., Higazi, M., Khurram, N., et al., (2021). Alpha-defensins: risk factor for thrombosis in COVID-19 infection. *Br. J. Haematol.*, **194**, 44–52.
63. Lehrer, R.I., Bevins, C.L., Ganz, T., (2005). Chapter 6 - Defensins and Other Antimicrobial Peptides and Proteins. In: Mestecky, J., Lamm, M.E., McGhee, J.R., Bienenstock, J., Mayer, L., Strober, W. (Eds.), *Mucosal Immunology*,. third ed. Academic Press, Burlington, pp. 95–110.
64. Ahmed, A., Siman-Tov, G., Hall, G., Bhalla, N., Narayanan, A., (2019). Human antimicrobial peptides as therapeutics for viral infections. *Viruses*, **11**
65. Park, M.S., Kim, J.I., Lee, I., Park, S., Bae, J.Y., Park, M. S., (2018). Towards the application of human defensins as antivirals. *Biomol. Ther. (Seoul)*, **26**, 242–254.
66. Eade, C.R., Wood, M.P., Cole, A.M., (2012). Mechanisms and modifications of naturally occurring host defense peptides for anti-HIV microbicide development. *Curr. HIV Res.*, **10**, 61–72.
67. Gupta, P., Lackman-Smith, C., Snyder, B., Ratner, D., Rohan, L.C., Patton, D., et al., (2013). Antiviral activity of retrocyclin RC-101, a candidate microbicide against cell-associated HIV-1. *AIDS Res. Hum. Retroviruses*, **29**, 391–396.
68. Eade, C.R., Cole, A.L., Diaz, C., Rohan, L.C., Parniak, M. A., Marx, P., et al., (2013). The anti-HIV microbicide candidate RC-101 inhibits pathogenic vaginal bacteria without harming endogenous flora or mucosa. *Am. J. Reprod. Immunol.*, **69**, 150–158.
69. Schaal, J.B., Tran, D., Tran, P., Osapay, G., Trinh, K., Roberts, K.D., et al., (2012). Rhesus macaque theta defensins suppress inflammatory cytokines and enhance survival in mouse models of bacteremic sepsis. *PLoS ONE*, **7**, e51337

70. Owen, S.M., Rudolph, D.L., Wang, W., Cole, A.M., Waring, A.J., Lal, R.B., et al., (2004). RC-101, a retrocyclin-1 analogue with enhanced activity against primary HIV type 1 isolates. *AIDS Res. Hum. Retroviruses*, **20**, 1157–1165.
71. Wu, Z., Ericksen, B., Tucker, K., Lubkowski, J., Lu, W., (2004). Synthesis and characterization of human alpha-defensins 4–6. *J. Pept. Res.*, **64**, 118–125.
72. Wu, Z., Hoover, D.M., Yang, D., Boulegue, C., Santamaria, F., Oppenheim, J.J., et al., (2003). Engineering disulfide bridges to dissect antimicrobial and chemotactic activities of human beta-defensin 3. *Proc. Natl. Acad. Sci. USA*, **100**, 8880–8885.
73. Wu, Z., Powell, R., Lu, W., (2003). Productive folding of human neutrophil alpha-defensins in vitro without the pro-peptide. *J. Am. Chem. Soc.*, **125**, 2402–2403.
74. Trepte, P., Kruse, S., Kostova, S., Hoffmann, S., Buntru, A., Tempelmeier, A., et al., (2018). LuTHy: a double-readout bioluminescence-based two-hybrid technology for quantitative mapping of protein-protein interactions in mammalian cells. *Mol. Syst. Biol.*, **14**, e8071
75. Bairoch, A., (2018). The cellosaurus, a cell-line knowledge resource. *J. Biomol. Tech.*, **29**, 25–38.
76. Uphoff, C.C., Drexler, H.G., (2014). Detection of mycoplasma contamination in cell cultures. *Curr. Protoc. Mol. Biol.*, **106**